Polymer 156 (2018) 121–127

Contents lists available at ScienceDirect

Polymer

journal homepage: www.elsevier.com/locate/polymer

A novel low colored and transparent shape memory copolyimide and its durability in space thermal cycling environments

Hui Gao[a], Jinrong Li[a], Fang Xie[b], Yanju Liu[c], Jinsong Leng[a,*]

[a] Centre for Composite Materials and Structures, Harbin Institute of Technology, Harbin, 150080, People's Republic of China
[b] School of Naval Architecture and Ocean Engineering, Harbin Institute of Technology, Weihai, 264209, People's Republic of China
[c] Department of Astronautical Science and Mechanics, Harbin Institute of Technology, Harbin, 150001, People's Republic of China

HIGHLIGHTS

- A novel low colored and transparent shape memory copolyimide (SMcoPI) with good optical transmittance was synthesized.
- The high optical transmittance of SMcoPI is the results of the reduction of the charge transfer complex interactions.
- SMcoPIs exhibit excellent low and high temperature resistance in the ground-simulated space thermal cycling environments.

ARTICLE INFO

Keywords:
Shape memory polymers
Shape memory copolyimide
Optical transmittance
Molecular chain arrangements
Shape memory behaviors
Thermal cycling

ABSTRACT

Recently, shape memory polymers (SMPs) with high optical transmittance have been paid great attentions to endow the flexible optoelectronics with shape memory functions. Herein, a low colored and transparent shape memory copolyimide (SMcoPI) is obtained by suppressing the charge transfer complex interactions. The optical transmittance of the synthesized SMcoPI film could reach at ~86% at the wavelength of 450 nm, far higher than the nearly zero optical transmittance of yellow and brown Kapton H. The better optical transparency could be attributed to the loose molecular chain arrangements induced by the *meta*-substituted groups and flexible ether linkages. The glass transition temperature (T_g) range of the synthesized SMcoPI films is from 179 °C to 220 °C, which is higher than that of reported optically transparent SMPs. The effective decomposition temperature at the weight loss of 5 wt% is 517 °C, showing excellent thermal stability. The SMcoPI also demonstrated good shape memory behaviors with high shape recovery ratio (R_r, > 96%) and shape fixity ratio (R_f, > 97%). In addition, the SMcoPI could maintain high optical transmittance, good thermostability and excellent shape memory behaviors after the ground-stimulated space thermal cycling test for 250 h. The synthesized SMcoPI has application potentials in high temperature areas or optoelectronic devices.

1. Introduction

Among engineering polymers, aromatic polyimides (PIs) have been widely applied in heat insulators [1–3], fuel cells [4–7], gas separation [8–10], heaters [11,12], sensors [13,14], etc., due to their excellent mechanical properties and thermal and chemical stabilities. However, wholly aromatic PIs has poor solubility in common organic solvents due to the rigid molecular chains and strong interchain interactions, thus making the processing inconvenient and expensive [15–19]. The applications of fully aromatic PIs are also severely restricted in some fields where high optical transparency is basically required due to their deep color and poor optical transparency [20–25], which could be attributed to the strong intra-/inter-molecular charge transfer complex (CTC) interactions in the highly conjugated molecular structures [22,26–29]. Therefore, the studies on soluble and transparent PIs have attracted many attentions by researchers in past few decades. To improve the processability and optical transparency of PIs, many investigations has been carried out in modifying the molecular structures of PIs, including introduction of bulky pendant groups [18,30], high fluoride and sulfone structures [17,30–32], unsymmetrical and noncoplanar structures [16,32] or flexible linkages [33] into polyimide chains to suppress CTC interactions. These fabricated colorless and transparent PIs have been used as the substrates for displays [34,35], transistors [36], solar cells [37], and heaters [38,39].

Integrating shape memory functions with the optical transparency will enormously expand the applications of PIs. Using optically

* Corresponding author.
E-mail address: lengjs@hit.edu.cn (J. Leng).

https://doi.org/10.1016/j.polymer.2018.10.001
Received 5 June 2018; Received in revised form 29 September 2018; Accepted 3 October 2018
Available online 04 October 2018
0032-3861/

transparent shape memory PIs as the substrates for flexible electronics will meet the requirements of high temperature applications that traditional transparent shape memory polymers are not available [40–45]. In past ten years, shape memory polyimides (SMPIs) and their composite materials with adjustable T_g ranging of 140–323 °C have been well developed and the shape memory functions have been also investigated trough bending, stretching and twisting methods [46–53]. Those SMPIs will have attractive high temperature applications where active shape change is required [47,54]. However, most SMPIs have deep color and poor optical transparency besides the only optically transparent SMPI that fabricated by Xiao et al. [55] in 2016. The optical transparency of the reported SMPI is achieved by reducing the molar ratio of the diamine to dianhydride, which will lead to poor mechanical properties.

In this paper, SMcoPI films were fabricated while keeping constant molar ratio of diamine ((1,3-bis(3-aminophenoxy)benzene (BAB)/(4,4′-(1,1′-biphenyl-4,4′-diyldioxy)dianiline (BAPB)) to dianhydride (bis phenol A dianhydride (BPADA)) of 1:1 and solid content of 15 wt%. The SMcoPI films have high optical transparency, excellent thermo-mechanical properties, thermal stabilities, excellent shape memory performances and good thermal cycling resistant properties. The T_g range of the SMcoPI is 179 °C–220 °C and could be tuned through adjusting the molar ratio of BAB to BAPB. The basic performances of SMcoPI films were characterized and the possible mechanism of the high transmittance of SMcoPI film was discussed, which could be a reference for the development of other transparent SMPs. Moreover, the durability of the high transmittance of SMcoPI film in the simulated space thermal cycling environments was investigated.

2. Experimental

2.1. Synthesis of the low colored and transparent shape memory copolyimide films

The two-step polycondensation process is demonstrated in Scheme 1, and the synthetic procedures are described as follows (as illustrated in Fig. S1). Firstly, the BAB (Tokyo Chemical Industry Co. Ltd., Japan) and BAPB (Aladdin Industrial Co. Ltd., China) were fed into DMAc (Aladdin Industrial Co. Ltd., China) solvent successively and stirred at 20 °C until completely dissolved. Then, BPADA (Sigma-Aldrich Co. Ltd., USA) was added into the above solution and stirred for one day at 20 °C, thus a poly(amic acid) with high viscosity (PAA) was formed successfully. The above polycondensation procedure was finished under the protection of dry nitrogen. Lastly, PAA was degassed on vacuum dry chamber at 40 °C for 3 h and then cast onto the supporting plates and the imidization occurs inside the oven where the temperature was successively kept at 80 °C, 110 °C, 180 °C, 200 °C and 250 °C for 2 h each. The samples were peeled off glass substrates in warm water, and dried at 100 °C in the vacuum dry chamber for 30 min. SMcoPI film samples named A1, A2, A3 and A4 were synthesized with different molar ratio of BAB to BAPB. The basic properties of these samples were characterized and the characterization methods could be found in Supplementary Information. The molar ratio, molecular weights (M_n), polydispersities (PDI), densities (ρ) and T_g of those samples are summarized in Table 1.

2.2. Ground-simulated space thermal cycling experiments

The simulated thermal cycling experiments were carried out in the BZ11 thermal cycling chamber with a vacuum pressure $\leq 6.65 \times 10^{-3}$ Pa. The operating temperature ranged from +88 °C to −117 °C at a heating/cooling temperature gradient of 3 °C/min. Each thermal cycle lasted for about 13.4 h, including 5 h at constant +88 °C and −117 °C, respectively. The total number of thermal cycling was 18.5 and the whole test period was about 250 h.

3. Results and discussion

3.1. Chemical structures and molecular chain structures

ATR-FTIR spectra of the samples are illustrated in Fig. 1. There are three typical peaks of PIs, i.e., the stretching vibration of C—N—C at 1368 cm^{-1}, symmetric stretching of C═O at 1715 cm^{-1} and asymmetric stretching of C═O at 1782 cm^{-1}. Meanwhile, we cannot find the traces of carbonyl (C═O) peaks of isoimides at 1795-1820 cm^{-1} or 920-935 cm^{-1}, and cannot observe the carbonyl (C═O) stretching peaks of inter-chain imides at around 1675 cm^{-1} neither [53–56]. Hence, the samples were all fully imidized after the second polycondensation process.

Judging from M_n and the structural unit (as illustrated in Scheme 1), the copolyimide chain of A2 comprises 120 structural units (m = 48, n = 72), where the repeat units are 24. Sample A2 has the larger structural unit number and higher distortion of copolyimide chains, since it has the highest M_n and PDI according to Table 1. The XRD patterns of the samples are shown in Fig. 2. The broad peaks of samples indicate that these samples are non-crystalline structures since the diffraction of intermolecular packing has some regularity combined with amorphous halo [22,55]. The amorphous nature of these SMPIs could be due to the introduction of the ether linkages and isopropylidene groups of BPADA and the *meta*-substituted ether linkages of BAB and BAPB. The broad peaks centered 2θ = 17.3°, 16.7°, 17.2° and 17.6°, for A1, A2, A3, A4, respectively, and the calculated interchain distances (d-spacing) were 5.1 Å, 5.3 Å, 5.1 Å, 4.9 Å. The larger interchain distance indicates that A2 might have looser polymer chain

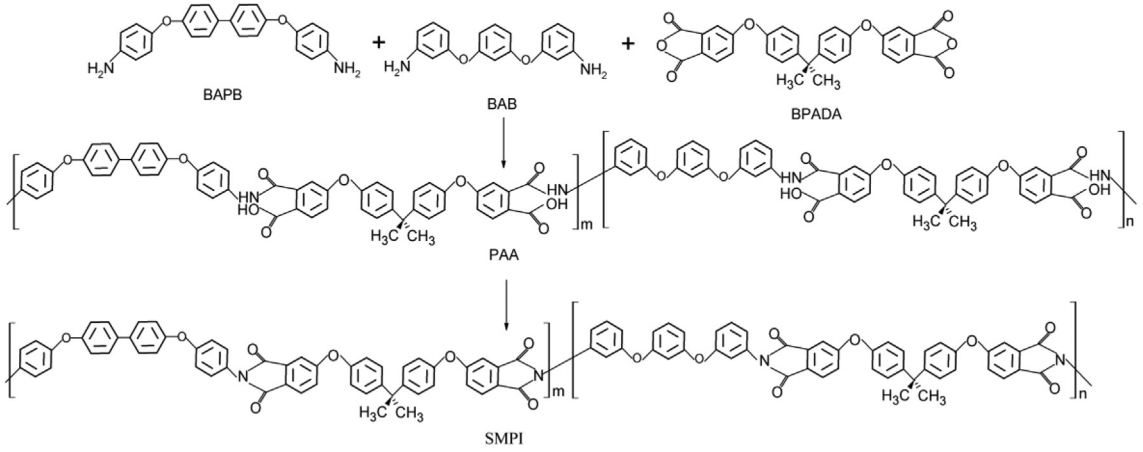

Scheme 1. The two-step polycondensation process of SMcoPI films.

Table 1
Performances of the samples with different T_g.

Title	Molar ratio (BAB:BAPB)	M_n (Kg/mol)	PDI	ρ (g/cm^3)	E' (MPa) at 25 °C	E' (MPa) at T_g-20 °C	E' (MPa) at T_g+20 °C	T_g (°C) by DMA	T_g (°C) by DSC
A1	0.95:0.05	81.65	1.43	1.2852 ± 0.001	2541 ± 39	1996 ± 14	4 ± 0.1	180 ± 1.7	165 ± 1.5
A2	0.60:0.40	96.98	1.51	1.2375 ± 0.001	1959 ± 18	1267 ± 22	8 ± 1.0	196 ± 1.0	182 ± 0.8
A3	0.20:0.80	87.49	1.41	1.2860 ± 0.001	2326 ± 23	863 ± 35	6 ± 0.1	212 ± 0.6	201 ± 0.5
A4	0.05:0.95	65.05	1.35	1.2976 ± 0.002	2454 ± 17	773 ± 29	6 ± 0.5	220 ± 1.5	214 ± 1.0

packing and aggregation [22,28,57], than the others. This could also be verified by the lowest density of A2, whose M_n is largest in all the samples (Table 1) [57]. The loose polyimide chain packaging and aggregation is beneficial to improve the polyimides' optical transparency [20–24] and this would be further discussed in Section 3.2.

Table 2 shows the solvent-resistance performances of samples. They can not only be dissolved in solvent with high-boiling point, like DMAc, N, N-dimethylformamide (DMF) and N-methyl pyrrolidone (NMP), but also in low-boiling point solvent, such as trichloromethane (CHCl3), n-Hexane and tetrahydrofuran (THF). The results show that SMcoPIs have good solubility in common organic solvents, which makes the post-processing convenient. Besides, we conclude from Table 2 that the solubility of samples in DMF and THF solvents shows a decrease trend with the increase of BAPB content, owing to the strong rigidity and intermolecular force of BAPB. By contrast, the samples have good resistance against frequently-used cleaning solvents like ethyl alcohol, acetone, and methylbenzene (PhMe), which is helpful in the fabrication of optoelectronic devices with the SMcoPI substrates.

3.2. Optical performances

The optical transmittances of the samples are illustrated in Fig. 3 and the inset optical photographs show that the highly transparent SMcoPI is light colored. The transmittance of A1, A2, A3 and A4 under 450 nm light is 50%, 86%, 46% and 35%, respectively. A2 has the highest optical transparency among those SMcoPI films, which could be explained by the previous conclusion of looser polymer chain packing of A2. At a wavelength of 450 nm–1100 nm, the light transmittance of A2 can reach up to 90%, indicating application potential in high-tech flexible electronics.

The possible mechanism of the suppression of the intramolecular CTC interactions, which leads to the increase of the samples' optical transparency, is described as follows. (1) The diamines and dianhydride both have *meta*-substituted groups and flexible R-O-R linkages that can decrease charge flow; (2) The molecular chains would fold and distort, after *meta*-substitution; (3) The pendant R2C(CH3)2 groups in BPADA could enlarge the molecular chains' free volume and prevent molecules from close contact; (4) The combination of R2C(CH3)2 groups and R-O-R linkages in BPADA could obstruct the main chain charge flow; (5) Copolycondensation with two diamines and one dianhydride could increase the distortion of molecular chains and break the π-π interactions.

3.3. Thermomechanical and thermal performances

The curves of storage modulus (E') and loss factor (tan δ) at varying temperatures are shown in Fig. 4. E' was high at glassy state and decreased slowly with the rise of temperature until a huge and sharp decrease in E' around T_g, and then the value of E' was very low at rubbery sate. The E' of the samples at 25 °C, T_g-20 °C and T_g+20 °C are listed in Table 1. The T_g of the samples, taken as the temperature corresponding to the peak of tan δ, is 179 °C, 196 °C, 212 °C and 220 °C, respectively, higher than that of other reported transparent SMPs [55]. We also tested the T_g of each sample through DSC, and the DSC curve is illustrated in Fig. S4. From Table 1, we can obtain the following facts: (a) E' of the samples with different BAPB content is almost the same in glassy state; (b) In intermediate state, E' shows a decrease trend with the increase of BAPB content, while, an opposite trend exists in rubbery state; (c) T_g increases with the increase of BAPB content. The sample A2 has the lowest E' at glassy state since the looser chain packaging and aggregation makes the molecular chain move more easily and thus improves the deformability.

Fox Equation can be used to characterize the relationship between T_g and content of the copolymers. For the low colored and transparent SMcoPI films, the T_g as a function of BAPB content in BPADA/BAB + BAPB copolyimide are expressed by Equation (1):

$$\frac{1}{T_g} = \frac{x_1}{T_{g,1}} + \frac{1 - x_1}{T_{g,2}} \quad (1)$$

Where, T_g, $T_{g,1}$ and $T_{g,2}$ represent the T_g of BPADA/BAB + BAPB copolyimide, pure BPADA/BAPB polyimide and pure BPADA/BAB polyimide, and x_1 and 1-x_1 represent the corresponding mass fraction of BAPB and BAB in BPADA/BAB + BAPB copolyimide. The predicted glass transition temperatures (T_gp) and the DMA results of SMcoPIs with different BAPB content are plotted in Fig. 5 and the predicted results coincide the DMA results with the Adj. R-Square of 0.992.

Thermal stabilities of the samples were tested by TGA/DSC instrument, and a series of TG and derivative thermogravimetic (DTG) curves

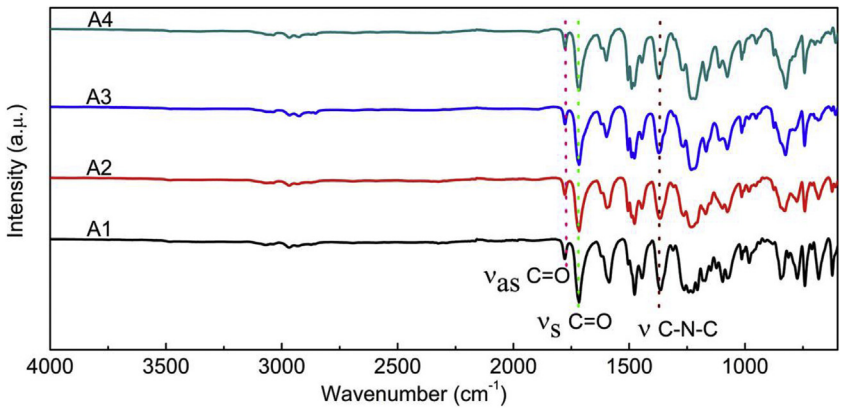

Fig. 1. ATR-FTIR spectra of A1, A2, A3 and A4.

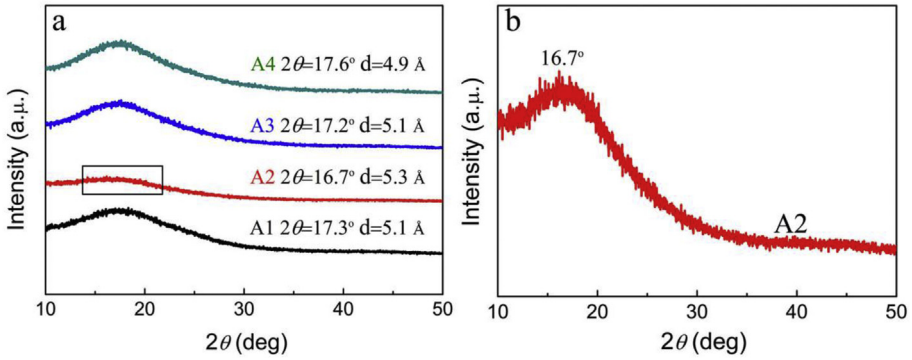

Fig. 2. (a) XRD spectra of the samples, and (b) the separate XRD spectra of A2.

Table 2
The solvent-resistance of SMcoPI films.

Sample	Solvent									
	Alcohol	PhMe	Acetone	DMF	DMAc	NMP	DMSO	CHCl3	THF	n-Hexane
A1	–	–	–	+ +	+ +	+ +	–	+ +	+ +	+ +
A2	–	–	–	+ +	+ +	+ +	–	+ +	+ +	+ +
A3	–	–	–	+	+ +	+ +	–	+ +	+	+ +
A4	–	–	–	+	+ +	+ +	–	+ +	+	+ +

Note: + + = Soluble(> 10%), + = Partially soluble(1–10%)– = Insoluble(< 1%).

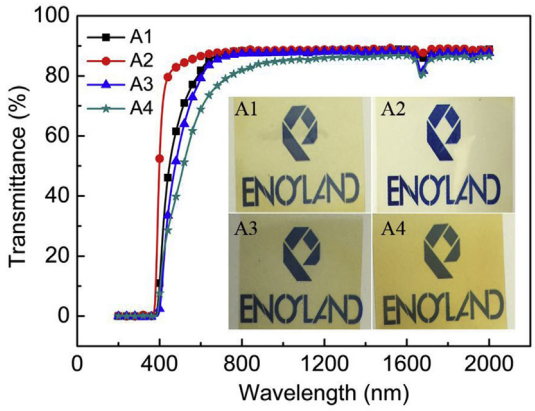

Fig. 3. The optical transmittance of the samples, and the inset shows their optical photographs.

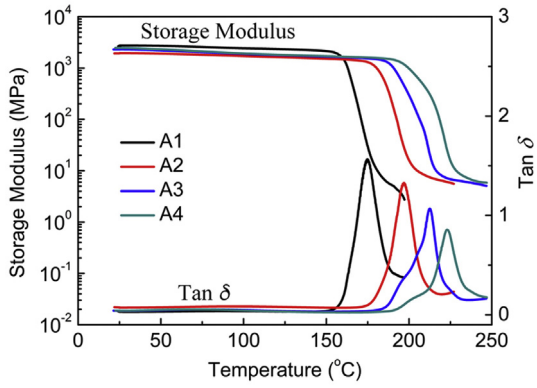

Fig. 4. Results of E' and tan δ as a function of temperature for samples.

are illustrated in Fig. S5. The effective decomposition temperature (T_d) at the weight loss of 5 wt% and T_{max} at the maximum weight loss of all the samples are all around 517 °C and 540 °C, respectively. There is about 50 wt% carbonaceous char left at 1000 °C. These results indicate that those SMcoPI films can work at high temperatures.

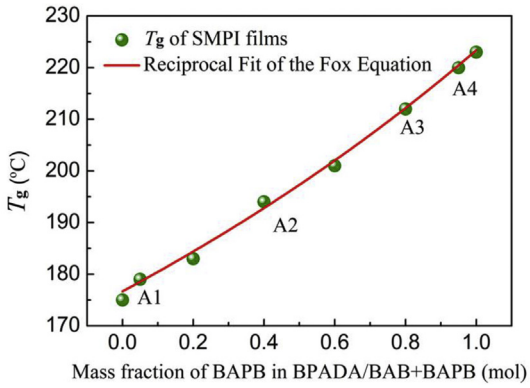

Fig. 5. T_gp of BPADA/BAB + BAPB copolyimides at different BAPB content.

3.4. Shape recovery performances

The deployable and stretchable shape recovery performances of the samples were tested and the shape recovery ratio (R_r) and shape fixity ratio (R_f) were calculated as described in Supplementary Information. The deployable R_f and R_r of the samples with the thickness of 100 μm are both higher than 99%, as illustrated in Fig. 6(a). In addition, the relationship between R_r and heating time was investigated and illustrated in Fig. 6(b). We can see that the samples could recover to the permanent shapes in 25 s. Those results demonstrate that the samples have excellent shape memory behaviors. The stretchable shape recovery curves of all samples are illustrated in Fig. 7, and the calculated results of the third stretchable shape memory cycle of all samples are listed in Table 3. The low colored and transparent SMcoPI films show excellent stretchable shape memory behaviors with R_f and R_r are both higher than 97% and 96%, respectively. It is mainly due to the large and sharp decrease in the E' around T_g, which is crucial for a good shape memory material [54]. Thus SMcoPI films could be used for shape programming as other shape memory polymers.

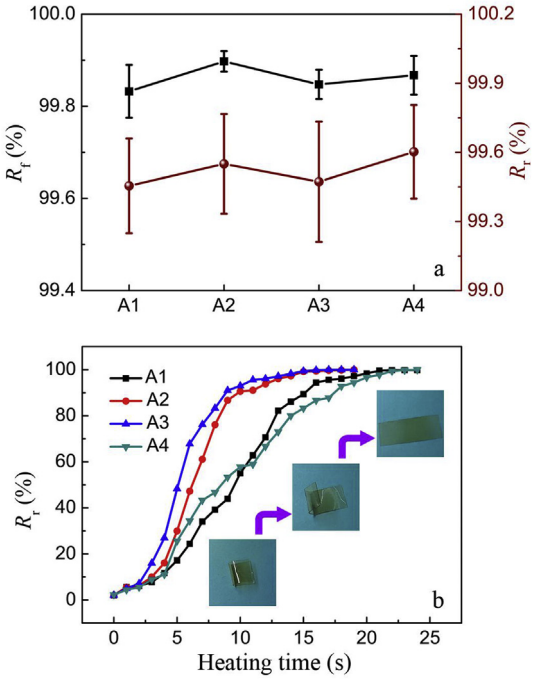

Fig. 6. (a) The deployable R_f and R_r of the samples and (b) the relationship between R_r of the samples and heating time, and the inset optical photographs show the bending shape recovery processes of A2.

3.5. The durability of the high transmittance of SMcoPI film in the space thermal cycling environments

FTIR-ATR spectra of A2 before and after thermal cycling (Fig. 8(a)) illustrate that the characteristic peaks of all functional groups of A2 remain unchanged after thermal cycling. Moreover, no new functional groups were produced after thermal cycling. The optical transmittance of A2, as illustrated in Fig. 8(b), shows a little reduction under thermal cycling. The TG and DMA curves of A2 before and after thermal cycling are almost overlapped, as illustrated in Fig. 8(c) and (d), indicating no obvious changes in the thermomechanical and thermal properties of the samples after thermal cycling. After being irradiated for 18.5 thermal cycles, sample A2 can completely recover from the programmed U-shape to the permanent shape under a hot plate in 25 s, as shown in Fig. 8(e). The stretchable shape recovery curve of A2 after thermal cycling is shown in Fig. 8(f). The calculated R_f and R_r of A2 after thermal cycling are also listed in Table 3 for comparison. Comparing the original and irradiated samples, R_f increased slightly while R_r decreased after thermal cycling. These results show that the low colored and transparent SMcoPI films could be durably utilized as thermal protective materials and in active deformation structures or deployable electronics with no detectable damages of molecular structures, optical transparency, shape memory behaviors, thermomechanical and even thermal properties.

Table 3
Stretchable shape memory performances of the samples.

Title	R_f (%)	R_r (%)
A1	97.95	96.20
A2	97.21	100.0
A2 after thermal cycling	97.55	97.30
A3	97.50	96.11
A4	97.07	96.80

4. Conclusions

In this paper, low colored and transparent SMcoPI films were synthesized through suppressing the charge transfer complex interactions by employing two diamines and dianhydride that contain *meta*-substituted groups and flexible ether linkages. The characterizations show that the samples have excellent thermal stability (T_d: ~517 °C, T_{max}: ~540 °C), excellent shape memory behavior (R_r > 96%, R_f > 97%), and good solubility in common solvents. The sample demonstrates optimal optical transmittance (~86% at the wavelength of 450 nm) when the molar ratio of BAB to BAPB is 0.6: 0.4. The high optical transmittance of such material is mainly the results of the packing and aggregation of loose molecular chains which is originated from the special copolyimides structures. The flexible ether linkage and *meta*-substituted structures could also greatly influence on the molecular chain arrangements and charge transfer complex interactions, ensuring the highly optical transmittance of SMcoPI film. The T_g of SMcoPI films ranges from 179 °C to 220 °C which is higher than that of previously-

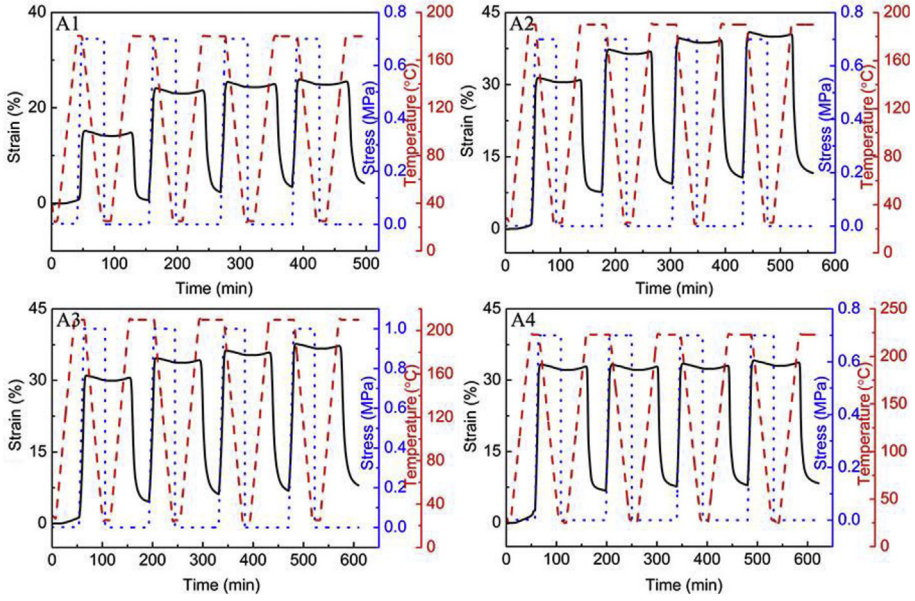

Fig. 7. The cycling shape recovery curves of samples with two-dimensional demonstration of changes in strain, stress and temperature versus time.

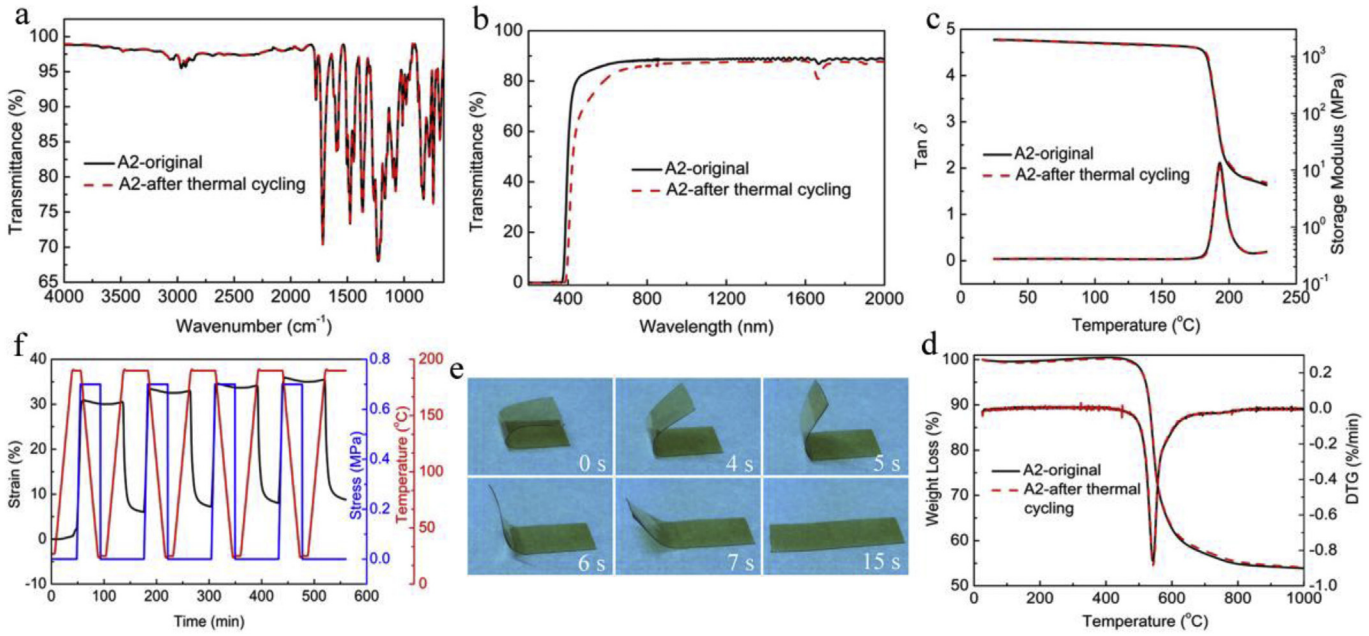

Fig. 8. (a) ATR-FTIR spectra, (b) optical transmittance, (c) thermomechanical properties, and (d) thermal stability of A2 before and after thermal cycling; The bending shape recovery images (e) and stretching shape recovery curves (f) of A2 after thermal cycling.

reported highly optically transparent SMPs. The low colored and transparent SMcoPI films could maintain their good chemical structures, optical transparency, thermomechanical properties, thermal stabilities and shape memory behaviors in space thermal cycling environments, showing some application potentials in the controllable deployment structures, thermal-protective materials and large-area solar cell arrays.

Acknowledgment

This work was supported by the National Natural Science Foundation of China (Grant No. 11632005, 11672086) and the Foundation for Innovative Research Groups of the National Natural Science Foundation of China (Grant No. 11421091).

Appendix A. Supplementary data

Supplementary data to this article can be found online at https://doi.org/10.1016/j.polymer.2018.10.001.

References

[1] J. Kwon, J. Kim, D. Park, H. Han, A novel synthesis method for an open-cell microsponge polyimide for heat insulation, Polymer 56 (2015) 68–72.
[2] Z. Qian, Z. Wang, Y. Chen, S. Tong, M. Ge, N. Zhao, J. Xu, Superelastic and ultralight polyimide aerogels as thermal insulators and particulate air filters, J. Mater. Chem. 6 (3) (2018) 828–832.
[3] F. Zhang, C. Tuck, R. Hague, Y. He, E. Saleh, Y. Li, C. Sturgess, R. Wildman, Inkjet printing of polyimide insulators for the 3D printing of dielectric materials for microelectronic applications, J. Appl. Polym. Sci. 133 (18) (2016) 43361.
[4] J. Lee, C.L. Lee, K. Park, I.D. Kim, Synthesis of an Al2O3-coated polyimide nanofiber mat and its electrochemical characteristics as a separator for lithium ion batteries, J. Power Sources 248 (2014) 1211–1217.
[5] H. Banda, D. Damien, K. Nagarajan, M. Hariharan, M.M. Shaijumon, A polyimide based all-organic sodium ion battery, J. Mater. Chem. 3 (19) (2015) 10453–10458.
[6] H.Q. Pham, G. Kim, H.M. Jung, S.W. Song, Fluorinated polyimide as a novel high-voltage binder for high-capacity cathode of lithium-ion batteries, Adv. Funct. Mater. 28 (2) (2018) 1704690.
[7] N. Zin, K. McIntosh, S. Bakhshi, A. Vázquez-Guardado, T. Kho, K. Fong, M. Stocks, E. Franklin, A. Blakers, Polyimide for silicon solar cells with double-sided textured pyramids, Sol. Energy Mater. Sol. Cell. 183 (2018) 200–204.
[8] M.Z. Ahmad, V. Martin-Gil, V. Perfilov, P. Sysel, V. Fila, Investigation of a new copolyimide, 6FDA-bisP and its ZIF-8 mixed matrix membranes for CO_2/CH_4 separation, Separ. Purif. Technol. 207 (2018) 523–534.
[9] X. Ma, M. Abdulhamid, X. Miao, I. Pinnau, Facile synthesis of a hydroxyl functionalized tröger's base diamine: a new building block for high-performance polyimide gas separation membranes, Macromolecules 50 (24) (2017) 9569–9576.
[10] N. Jusoh, Y.F. Yeong, K.K. Lau, A.M. Shariff, Enhanced gas separation performance using mixed matrix membranes containing zeolite T and 6FDA-durene polyimide, J. Membr. Sci. 525 (2017) 175–186.
[11] S. Khan, T.P. Nguyen, M. Lubej, L. Thiery, P. Vairac, D. Briand, Low-power printed micro-hotplates through aerosol jetting of gold on thin polyimide membranes, Microelectron. Eng. 194 (2018) 71–78.
[12] P. Li, J. Ma, H. Xu, X. Xue, Y. Liu, Highly stable copper wire/alumina/polyimide composite films for stretchable and transparent heaters, J. Mater. Chem. C 4 (16) (2016) 3581–3591.
[13] Y. Qin, Q. Peng, Y. Ding, Z. Lin, C. Wang, Y. Li, F. Xu, J. Li, Y. Yuan, X. He, Y. Li, Lightweight, superelastic, and mechanically flexible graphene/polyimide nanocomposite foam for strain sensor application, ACS Nano 9 (9) (2015) 8933–8941.
[14] C. Cheng, S. Wang, J. Wu, Y. Yu, R. Li, S. Eda, J. Chen, G. Feng, B. Lawrie, A. Hu, Bisphenol a sensors on polyimide fabricated by laser direct writing for onsite river water monitoring at attomolar concentration, ACS Appl. Mater. Interfaces 8 (28) (2016) 17784–17792.
[15] Y. Liu, X. Qian, H. Shi, W. Zhou, Y. Cai, W. Li, H. Yao, New poly(amide-imide)s with trifluoromethyl and chloride substituents: synthesis, thermal, dielectric, and optical properties, Eur. Polym. J. 94 (2017) 392–404.
[16] L.R. Sidra, G. Chen, C. Li, N. Mushtaq, K. Ma, X. Fang, Processable, high T_g polyimides from unsymmetrical diamines containing 4-phenoxy aniline and benzimidazole moieties, Polymer 148 (2018) 228–238.
[17] P.K. Tapaswi, M.C. Choi, S. Nagappan, C.S. Ha, Synthesis and characterization of highly transparent and hydrophobic fluorinated polyimides derived from perfluorodecylthio substituted diamine monomers, J. Polym. Sci., Polym. Chem. Ed. 53 (3) (2015) 479–488.
[18] S.D. Kim, S. Lee, H.S. Lee, S.Y. Kim, I.S. Chung, New soluble polyamides and polyimides containing polar functional groups: pendent pyrazole rings with amino and cyano groups, Des. Monomers Polym. 19 (3) (2016) 227–235.
[19] Y. Guan, C. Wang, D. Wang, G. Dang, C. Chen, H. Zhou, X. Zhao, High transparent polyimides containing pyridine and biphenyl units: synthesis, thermal, mechanical, crystal and optical properties, Polymer 62 (2015) 1–10.
[20] M. Hasegawa, K. Horie, Photophysics, photochemistry, and optical properties of polyimides, Prog. Polym. Sci. 26 (2) (2001) 259–335.
[21] M.C. Choi, J.C. Hwang, C. Kim, S. Ando, C.S. Ha, New colorless substrates based on polynorbornene-chlorinated polyimide copolymers and their application for flexible displays, J. Polym. Sci., Polym. Chem. Ed. 48 (8) (2010) 1806–1814.
[22] L. Zhai, S. Yang, L. Fan, Preparation and characterization of highly transparent and colorless semi-aromatic polyimide films derived from alicyclic dianhydride and aromatic diamines, Polymer 53 (16) (2012) 3529–3539.
[23] H. Seino, T. Sasaki, A. Mochizuki, M. Ueda, Synthesis of fully aliphatic polyimides, High Perform. Polym. 11 (3) (1999) 255–262.
[24] Y. Watanabe, Y. Sakai, M. Ueda, Y. Oishi, K. Mori, Synthesis of wholly alicyclic polyimides from N-silylated alicyclic diamines, Chem. Lett. 29 (5) (2000) 450–451.
[25] A.S. Mathews, I. Kim, C.S. Ha, Synthesis and characterization of novel fully aliphatic polyimidosiloxanes based on alicyclic or adamantly diamines, J. Polym. Sci., Polym. Chem. Ed. 44 (18) (2006) 5254–5270.
[26] W. Chen, Z. Zhou, T. Yang, R. Bei, Y. Zhang, S. Liu, Z. Chi, X. Chen, J. Xu, Synthesis

and properties of highly organosoluble and low dielectric constant polyimides containing non-polar bulky triphenyl methane moiety, React. Funct. Polym. 108 (2016) 71–77.
[27] K.H. Nam, H. Kim, H.K. Choi, H. Yeo, M. Goh, J. Yu, J.R. Hahn, H. Han, B.C. Ku, N.H. You, Thermomechanical and optical properties of molecularly controlled polyimides derived from ester derivatives, Polymer 108 (2017) 502–512.
[28] Z. Mi, Z. Liu, J. Yao, C. Wang, C. Zhou, D. Wang, X. Zhao, H. Zhou, Y. Zhang, C. Chen, Transparent and soluble polyimide films from 1,4:3,6-dianhydro-D-mannitol based dianhydride and diamines containing aromatic and semiaromatic units: preparation, characterization, thermal and mechanical properties, Polym. Degrad. Stabil. 151 (2018) 80–89.
[29] M. Hasegawa, T. Ishigami, J. Ishii, Optically transparent aromatic poly(ester imide)s with low coefficients of thermal expansion (1). Self-orientation behavior during solution casting process and substituent effect, Polymer 74 (2015) 1–15.
[30] S. Dal Kim, S. Lee, J. Heo, S.Y. Kim, I.S. Chung, Soluble polyimides with trifluoromethyl pendent groups, Polymer 54 (21) (2013) 5648–5654.
[31] L. Akbarian-Feizi, S. Mehdipour-Ataei, H. Yeganeh, Investigation on the preparation of new sulfonated polyimide fuel cell membranes in organic and ionic liquid media, Int. J. Polym. Mater. 63 (3) (2014) 149–160.
[32] C.Y. Wang, G. Li, J.M. Jiang, Synthesis and properties of fluorinated poly(ether ketone imide)s based on a new unsymmetrical and concoplanar diamine: 3,5-Dimethyl-4-(4-amino-2-trifluoromethylphenoxy)-4′-aminobenzophenone, Polymer 50 (7) (2009) 1709–1716.
[33] N. Amutha, S.A. Tharakan, M. Sarojadevi, Synthesis and characterization of new soluble polyimides based on pyridine unit with flexible linkages, High Perform. Polym. 27 (8) (2015) 979–989.
[34] H. Lim, W.J. Cho, C.S. Ha, S. Ando, Y.K. Kim, C.H. Park, K. Lee, Flexible organic electroluminescent devices based on fluorine-containing colorless polyimide substrates, Adv. Mater. 14 (18) (2002) 1275–1279.
[35] L. Qu, L. Tang, R. Bei, J. Zhao, Z. Chi, S. Liu, X. Chen, M.P. Aldred, Y. Zhang, J. Xu, Flexible multifunctional aromatic polyimide film: highly efficient photoluminescence, resistive switching characteristic, and electroluminescence, ACS Appl. Mater. Interfaces 10 (14) (2018) 11430–11435.
[36] Y.Y. Yu, T.J. Huang, W.Y. Lee, Y.C. Chen, C.C. Kuo, Highly transparent polyimide/nanocrystalline-zirconium dioxide hybrid materials for organic thin film transistor applications, Org. Electron. 48 (2017) 19–28.
[37] J.I. Park, J.H. Heo, S.H. Park, K.I. Hong, H.G. Jeong, S.H. Im, H.K. Kim, Highly flexible InSnO electrodes on thin colourless polyimide substrate for high-performance flexible CH3NH3PbI3 perovskite solar cells, J. Power Sources 341 (2017) 340–347.
[38] J.H. Lee, D.Y. Youn, Z. Luo, J.Y. Moon, S.J. Choi, C. Kim, I.D. Kim, Cu microbelt network embedded in colorless polyimide substrate: flexible heater platform with high optical transparency and superior mechanical stability, ACS Appl. Mater. Interfaces 9 (45) (2017) 39650–39656.
[39] Q. Huang, W. Shen, X. Fang, G. Chen, J. Guo, W. Xu, R. Tan, W. Song, Highly flexible and transparent film heaters based on polyimide films embedded with silver nanowires, RSC Adv. 5 (57) (2015) 45836–45842.
[40] J. Reeder, M. Kaltenbrunner, T. ware, D. Arreaga-Salas, A. Avendano-Bolivar, T. Yokota, Y. Inoue, M. Sekino, W. Voit, T. Sekitani, T. Someya, Mechanically adaptive organic transistors for implantable electronics, Adv. Mater. 26 (29) (2014) 4967–4973.
[41] T. Ware, D. Simon, K. Hearon, C. Liu, S. Shah, J. Reeder, N. Khodaparast, M.P. Kilgard, D.J. Maitland, R.L. Rennaker II, W.E. Voit, Three-dimensional flexible electronics enabled by shape memory polymer substrates for responsive neural interfaces, Macromol. Mater. Eng. 297 (12) (2012) 1193–1202.
[42] H. Xu, C. Yu, S. Wang, V. Malyarchuk, T. Xie, J.A. Rogers, Deformable, programmable, and shape-memorizing micro-optics, Adv. Funct. Mater. 23 (26) (2013) 3299–3306.
[43] P. Li, Y. Han, W. Wang, Y. Liu, P. Jin, J. Leng, Novel programmable shape memory polystyrene film: a thermally induced beam-power splitter, Sci. Rep.-UK 7 (2017) 44333.
[44] M.P. Gaj, A. Wei, C. Fuentes-Hernandez, Y. Zhang, R. Reit, W. Voit, S.R. Marder, B. Kippelen, Organic light-emitting diodes on shape memory polymer substrates for wearable electronics, Org. Electron. 25 (2015) 151–155.
[45] Z. Yu, Q. Zhang, L. Li, Q. Chen, X. Niu, J. Liu, Q. Pei, Highly flexible silver nanowire electrodes for shape-memory polymer light-emitting diodes, Adv. Mater. 23 (5) (2011) 664–668.
[46] X. Xiao, D. Kong, X. Qiu, W. Zhang, F. Zhang, L. Liu, Y. Liu, S. Zhang, Y. Hu, J. Leng, Shape-memory polymers with adjustable high glass transition temperatures, Macromolecules 48 (11) (2015) 3582–3589.
[47] X. Xiao, D. Kong, X. Qiu, W. Zhang, Y. Liu, S. Zhang, F. Zhang, Y. Hu, J. Leng, Shape memory polymers with high and low temperature resistant properties, Sci. Rep.-UK 5 (2015) 14137.
[48] D. Kong, X. Xiao, Rigid high temperature heat-shrinkable polyimide tubes with functionality as reducer couplings, Sci. Rep.-UK 7 (2017) 44936.
[49] Q. Wang, Y. Bai, Y. Chen, J. Ju, F. Zheng, T. Wang, High performance shape memory polyimides based on π–π interactions, J. Mater. Chem. 3 (1) (2015) 352–359.
[50] Y. Bai, L. Mao, Y. Liu, High temperature shape memory polyimide ionomer, J. Appl. Polym. Sci. 133 (30) (2016) 43630.
[51] M. Yoonessi, Y. Shi, D.A. Scheiman, M. Lebron-Colon, D.M. Tigelaar, R.A. Weiss, M.A. Meador, Graphene polyimide nanocomposites: thermal, mechanical, and high-temperature shape memory effects, ACS Nano 6 (9) (2012) 7644–7655.
[52] R. Biju, C.R. Nair, High transition temperature shape memory polymer composites based on bismaleimide resin, High Perform. Polym. 25 (4) (2013) 464–474.
[53] D. Kong, X. Xiao, High cycle-life shape memory polymer at high temperature, Sci. Rep.-UK 6 (2016) 33610.
[54] H. Gao, X. Lan, L. Liu, X. Xiao, Y. Liu, J. Leng, Study on performances of colorless and transparent shape memory polyimide film in space thermal cycling, atomic oxygen and ultraviolet irradiation environments, Smart Mater. Struct. 26 (9) (2017) 095001.
[55] X. Xiao, X. Qiu, D. Kong, W. Zhang, Y. Liu, J. Leng, Optically transparent high temperature shape memory polymers, Soft Matter 12 (11) (2016) 2894–2900.
[56] C.A. Pryde, IR studies of polyimides. I. Effects of chemical and physical changes during cure, J. Polym. Sci., Polym. Chem. Ed. 27 (2) (1989) 711–724.
[57] A. Wolinska-Grabczyk, E. Schab-Balcerzak, E. Grabiec, A. Jankowski, M. Matlengiewicz, U. Szeluga, P. Kubica, Structure and properties of new highly soluble aromatic poly(etherimide)s containing isopropylidene groups, Polym. J. 45 (12) (2013) 1202–1209.